Thermal conductivity in a one-dimensional Lennard-Jones chain by molecular dynamics

M. Mareschal and A. Amellal
Faculté des Sciences, Code Postale 231, Université Libre de Bruxelles, B1050, Brussels, Belgium
(Received 30 April 1987)

The existence of thermal conductivity is examined for a one-dimensional chain of Lennard-Jones particles, using techniques of equilibrium and nonequilibrium molecular dynamics. The transport of energy by soundlike pulses is related to the anomalous fluctuations of the heat flux in this model. Equilibrium time properties are governed by two time scales which can be measured. The effects of modifications to the original model are also examined: particles having different masses, eventually with different interaction potentials or under the influence of an external sinusoidal field.

I. INTRODUCTION

One-dimensional systems have always been the object of much interest in statistical mechanics. They provide simple models where complex phenomena can be analyzed in a precise way. This has also been the case for numerical studies; one of the first reports on molecular dynamics concerned the energy sharing among normal modes in a linear assembly of anharmonic oscillators.[1] From the point of view of molecular dynamics, one-dimensional systems are interesting for their low computational cost. Indeed the processing time needed to integrate the equations of motion increases as the number of particles, instead of its square in higher dimensionality. Numerical models with relatively large sizes can then be studied. They could be used, for example, to test the existence of long-range correlations in nonequilibrium states, a theoretical prediction[2] which has been difficult to confirm experimentally.[3] This was our motivation when we considered first the one-dimensional Lennard-Jones (LJ) chain.

However, the very existence of thermodynamic behavior is questionable in one dimension. Early studies of linear assemblies of harmonic oscillators[4] have shown that these models, although not dissipative, are able to spread initial disturbances at long times. The change in the spectral properties due to differences in the masses of the particles has also been examined.[5] The presence of anharmonic forces is known to be a necessary condition for dissipativity since the classical work of Peierls.[6] In one dimension, however, terms cubic in the anharmonicity are not sufficient for having finite transport coefficients and it can be argued that quartic terms, allowing four-phonon interactions (Umklapp processes), can bring dissipation in such models; there has always been, however, some doubt on the existence of thermal conductivity in one dimension,[7] and these doubts have been reinforced since the discovery of long-time tails in fluids and its explanation by mode-coupling theories.[8]

Numerical work, on the other hand, has been mainly devoted to the study of ergodic properties. For instance, Ford[9] found some explanation for the nonsharing among energy modes in the Fermi model. Other one-dimensional models did show equipartition provided the nonlinearity was strong enough.[10] The continuous limit of these nonlinear models has permitted to study the energy transport due to solitary waves.[11,12] In the one-dimensional Lennard-Jones system, a transition was found from ordered to stochastic trajectories.[13] That transition occurs at an energy per particle of a few percent of the well depth of the interaction potential energy.

More recently, Gillan and Holloway have examined the thermal conductivity of a one-dimensional undamped Frenkel-Kontorova model,[14] and they found a finite thermal conductivity, both by equilibrium and nonequilibrium molecular dynamics. The same was also found for a model consisting of hard rods on a line, 1 out of 2 of them being harmonically bound to a line node[15] (the randomness of the trajectories of this model lead the authors to propose to name it the "ding-a-ling" model). This last model did show a transition from near integrable to stochastic behavior as the frequency of the harmonic link is increased. In the ordered region, transport is mainly due to the solitary waves, whereas in the stochastic region diffusive behavior is observed. Let us also mention the work of Mokross and Buttner,[16] who have studied a one-dimensional diatomic Toda lattice by nonequilibrium molecular-dynamics methods: They found a linear temperature profile in nonequilibrium steady states, leading therefore to a measure of the heat conductivity. However, they did not compare their results to equilibrium measurements.

The presently reported work is concerned with the existence and measurement of thermal conductivity in a linear assembly of point particles interacting through the Lennard-Jones potential and should be considered as a phenomenological approach to this question. The density of particles is such that each particle, on the average, is at a distance corresponding to the minimum of the interaction potential so that it can be compared to an anharmonic chain. We used the techniques of nonequilibrium molecular dynamics, described, for instance, in Ref. 15, to observe how the system responds to an external constraint like thermal boundaries. Although the temperature profile measured on the system is linear and thus a conductivity can be measured, the fluctuations in this model look anomalous. We then turned to equilibrium measurements in order to observe if the fluctuations

of the heat flux could lead to dissipative (that is rapidly decaying in time) Green-Kubo integrands, as in the models studied in Refs. 14 and 15. An unexpected and interesting result is that the computation of the heat-flux correlation function shows a very slow decay in time, leading therefore to a divergence in the transport coefficient. We suggest to relate this behavior to the persistence of excitations in the model that propagate for a very long time before they are damped. As this has not been observed in, for instance, the "ding-a-ling" model, one can conclude that the dimensionality of the present model is not the only reason for the nonexistence of normal transport. The question that we have tried to analyze then is to characterize the mechanisms that allow the validity of the Fourier law in some one-dimensional models. Our approach has been intuitive and we have tried some modifications to the original model in order to make it more dissipative. This led us to consider the presence of impurities or that of an external field. This is described in more detail in the article itself, together with a discussion on the reasons for these modifications and the results obtained.

The article is organized as follows. The model is presented in Sec. II, together with the basic definitions required. In Sec. III we report on the nonequilibrium experiments; a brief description of the technique is given and then the results are presented. Section IV is devoted to the presentation of the equilibrium properties of the various models. These are discussed in Sec. V, together with some conclusions.

II. THE MODEL

The system consists of N point particles moving on a line of length L, whose curvature is neglected although, the system being periodic, it closes on itself. The total energy of the particles is

$$H=\sum_{i=1}^{N}\left[m_i v_i^2/2+\tfrac{1}{2}\sum_{j\neq i}V(x_{ij})\right], \tag{1}$$

where m_i is the mass of the ith particle, $v_i=dx_i/dt$ its velocity, and $V(x_{ij})$, the potential of the interactions forces, is of the Lennard-Jones type:

$$V(x_{ij})=4\epsilon[(\sigma/x_{ij})^{12}-(\sigma/x_{ij})^{6}]\ . \tag{2}$$

In the simple model, all masses are taken to be the same, m. As usual,[17] we choose units in which ϵ is 1, σ is 1, and the mass m is equal to 48. The equations of motion for the system are numerically solved with the Verlet algorithm;[18] in our units, the time step is taken to be 0.032, which corresponds to one hundredth of a "collision" time. The system is divided in cells containing typically 10 particles. In these cells, one measures particle and energy densities as local time averages. We have also measured the velocity distribution function, and, in particular, its second moment is related to the temperature through

$$(k_B T_\alpha/2)=\left[\sum_{i\in\alpha} m_i v_i^2/2\right]\Big/\left[\sum_{i\in\alpha}1\right]. \tag{3}$$

The summation on particles i extends over all the particles which belong to the cell a, and the right-hand side of Eq. (3) is the ratio of two time averages. This definition has been used in nonequilibrium stationary states to measure the temperature profile in the chain.

Another quantity of interest is, of course, the heat flux. The energy density is defined as usual as

$$e(x,t)=\sum_{i=1}^{N}\left[m_i v_i^2/2+\tfrac{1}{2}\sum_{j\neq i}V(x_{ij})\right]\delta(x_i(t)-x)\ . \tag{4}$$

We then derive the energy density with respect to time in order to find the local conservation equation

$$\frac{de(x,t)}{dt}+\frac{dJ_q(x,t)}{dx}=0\ . \tag{5}$$

One easily finds the form for the heat flux:

$$J_q(x,t)=\sum_{i=1}^{N} v_i\left[m_i v_i^2/2+\tfrac{1}{2}\sum_{j\neq i}V(x_{ij})\right]\delta(x_i(t)-x) -\tfrac{1}{2}\sum_{i\neq j}\frac{dV(x_{ij})}{dx_{ij}}x_{ij}v_i\alpha\left[x_{ij}\frac{d}{dx}\right] \times\delta(x_i(t)-x)\ , \tag{6}$$

where $\alpha(x)=(e^x-1)/x$. We are interested in the hydrodynamic contribution to this quantity; that is we consider distances which are great with respect to the interatomic distances. In this limit, we expand the α operator, and we are left with

$$J_q(t)=\frac{1}{L}\sum_{i=1}^{N} v_i\left[m_i v_i^2/2+\tfrac{1}{2}\sum_{j\neq i}V(x_{ij})\right] -\frac{1}{2L}\sum_{i\neq j}\frac{dV(x_{ij})}{dx_{ij}}x_{ij}v_i \tag{7}$$

for the total heat flux of the system. Notice that no mass flux has to be removed, as the total momentum is fixed initially to zero. It is interesting to note that this heat-flux definition is not modified by the presence of an external field:

$$V_{\text{field}}=\sum_{i=1}^{N}V_0\cos(2\pi x_i/a)\ , \tag{8}$$

where a is set equal to $2^{1/6}$, the average mean distance between particles, which is equal to L/N.

III. NONEQUILIBRIUM RESULTS

In order to maintain the system out of equilibrium, two opposite cells are chosen on the chain which will act as reservoirs. The velocities of the particles which belong to these cells are rescaled so that permanently the temperatures of these cells, as defined by Eq. (3), are fixed and different one from the other. As the algorithm is a second-order centered difference, involving only the positions and not the velocities, this scaling is introduced via the modification of the previous position of the particles belonging to the reservoir cells.

The systems considered consisted of 200 particles. They were put initially at an equilibrium distance one from the other and given velocities randomly chosen in a Gaussian distribution corresponding to an arbitrarily chosen temperature. In all the runs, the lower temperature was always set to 1, $k_B T_1 = 1$, in energy units where ϵ is 1, whereas the higher temperature was successively set to $k_B T_2 = 2$ and 20. The system is then integrated in time until a stationary state is reached for the temperature profile. This transient lasts for about 10 000 time steps. Then one measures the cells' temperature and number densities. We show the measurements of the temperature and density profiles for two different imposed temperature gradients in Figs. 1(a) and 1(b). The resulting temperature profile is linear with a temperature slip at the reservoirs, similar to what has been observed for fluids of higher dimensionality in similar experiments.[19] However, the temperature slip is much more important. In Table I we give the imposed temperature difference as compared to the measured one. The ratio of the imposed temperature gradient over the measured one is around 4. The local number density also varies and seems to be in equilibrium with the local temperature so as to maintain a constant pressure. We also show the velocity distribution function for two cells which are central in the system, between the two reservoir cells. The distribution is much affected by the nonequilibrium stationary heat flux which makes it asymmetric.

TABLE I. Effective vs imposed temperature gradients in nonequilibrium simulations. The measured temperature difference is calculated via linear fit. The heat conductivity is calculated through the ratio of the mean flux to the temperature gradient.

$(\Delta T/L)_{\text{imposed}}$	$(\Delta T/L)_{\text{measured}}$	T_{average}	λ/k_B
0.1	0.026	1.3	4.8
1.9	0.571	7.3	16.5

It is to be noted that another thermalization procedure was first used: instead of considering an entire cell as a reservoir, the thermalization consisted in the modification of the velocity of particles crossing a fictitious boundary. The sign of the velocity remained unchanged but its magnitude was chosen in a Gaussian distribution corresponding to the desired temperature. The effect on the system was to modify the velocity distribution function, with a discontinuity at $v = 0$. This is shown in Figs. 2 and 3, where we plot the velocity distribution functions for the two thermalizations mechanisms. As a matter of fact, the procedure which we previously used leads to tremendous changes in particles velocities. So that it often happened in the high-temperature reservoir, a large amount of energy was introduced in the system and was then transported without any mixing to the cold boundary where it could be absorbed. This can be seen in Fig. 4, where the energy density is represented as a function of space and time. The rescaled velocity is transported by collisions which exchange the velocities, like in hard-rod systems. The velocity distribution function separates into two populations of velocities: the positive, which corresponds to a high temperature, and the negative, corresponding to a smaller temperature. This is reminiscent of the behavior of gases in the Knudsen regime (that is, for gases having a mean free path of the order of the dimen-

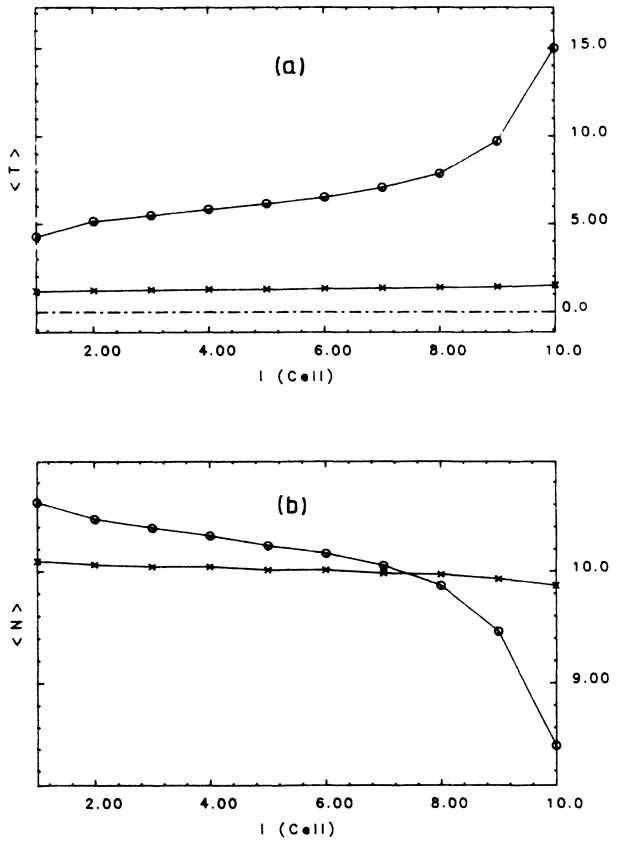

FIG. 1. Temperature and number density profiles in the nonequilibrium runs. Each point is the average of the two opposing cells which are symmetrical with respect to the constraint ($\times$, $\Delta T = 1$; $\circ$, $\Delta T = 19$).

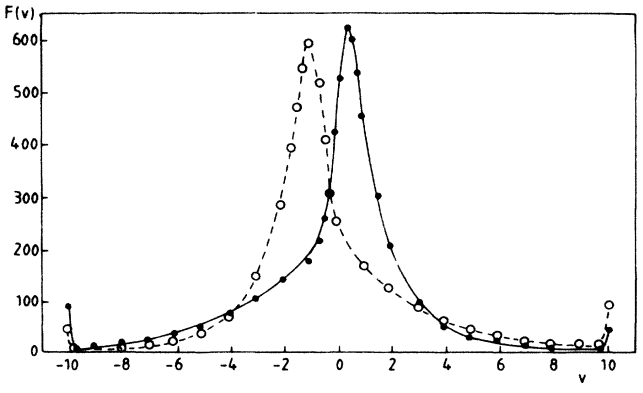

FIG. 2. Velocity distribution functions for the two central cells. The velocity space has been divided into 20 intervals; the function represents the number of particles in the given interval, accumulated during the entire run.

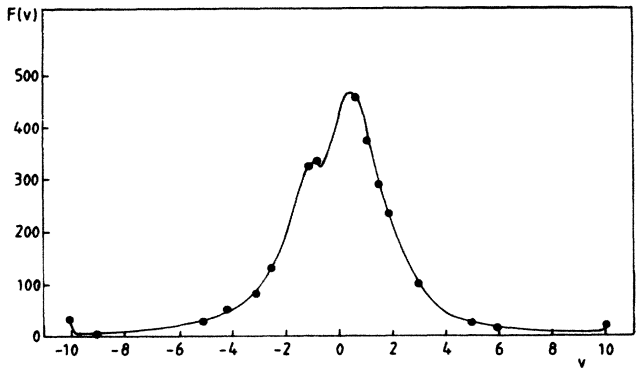

FIG. 3. Same as in Fig. 2, except for the thermalization mechanism. Here thermalization is achieved by changing the velocity of one particle at a time.

sions of the containing vessel) where no collision takes place; here the collisions result in the transport of unchanged momentum and energy, as for hard rods. Of course, the relevant mean free path here is the phonon mean free path which extends over many interparticle distances. The one-particle velocity scaling is a mechanism of thermalization which reinforces a pathology of the model: disturbances can be transported without deformation across the system. This type of behavior was shown to lead to solitary-waves transport (see Ref. 12). On scales of the order of the phonon mean free path, the local equilibrium assumption breaks down, and expansion around two half-Maxwellian should probably be more adapted. Indeed the measured moments of the distribution function do not satisfy the relations that Gaussian moments do, as is the case for the other thermalization mechanism.

With the cell thermalization mechanism, no such behavior was observed at the level of energy density or velocity distribution function. The nonequilibrium results

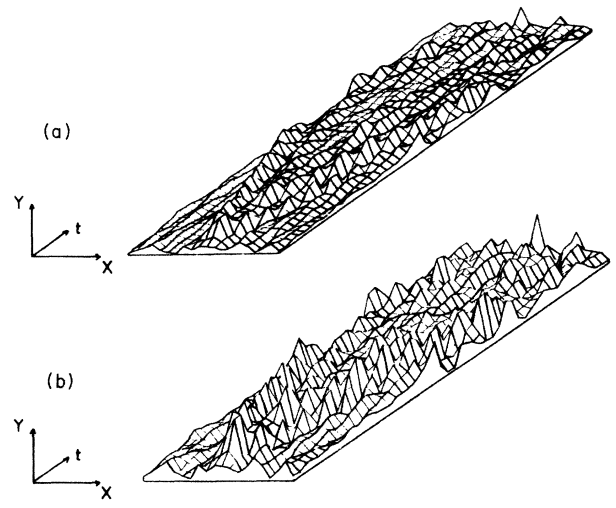

FIG. 4. Energy density as a function of time (depth) and cell position (front axis). Graph (a) is the kinetic energy density and graph (b) is the potential energy density.

suggest that, although the system seems able to propagate solitary waves, it is also dissipative enough to produce a temperature gradient opposing an external heat flux. We also looked at the fluctuations of the kinetic energy per particle per cell; a characteristic feature of these fluctuations is that the results obtained needed a very long time to stabilize, and that from one run to the other, significant differences could be found, leading to very large error bars.

IV. EQUILIBRIUM FLUCTUATIONS

In order to investigate if the capacity of the model to transport energy in the form of waves does affect its equilibrium properties as well, we also looked at its equilibrium fluctuations. Fluctuations of the kinetic energy are related to the heat capacity[20] in a microcanonical ensemble, as are the fluctuations of the heat flux related to the thermal conductivity through the Green-Kubo relation:[21]

$$\lambda=(1/Nk_BT^2)\int dt\langle J_q(t)J_q(0)\rangle \ . \tag{9}$$

Table II lists the equilibrium runs done for these systems and the heat capacities measured from the fluctuations of the mean kinetic energy per particle. The values of these are between the value of perfect gas ($C/k_B=1/2$) and those of harmonic oscillator ($C/k_B=1$). However, it should be noted also that the measured values did vary from one run to the other and that no general trends could be seen as for the dependency on the density or number of particles in the chain.

Most of the runs were done for a density $N/L=1/(2^{1/6})$ and for 200 particles. The initial state was that of equidistant particles with velocities chosen in a Gaussian distribution corresponding to a temperature double of what should be reached; we set the temperature equal to 0.7 and this corresponds to a state with approximately equal potential and kinetic energies. Some runs were done for larger systems ($N=1000$), and smaller densities. No number dependence could be seen in the time behavior of the heat flux. This quantity is shown in Fig. 5; each point of this graph is an average over 100 time steps, so that the figure corresponds to a run of 200 000 time steps. Obviously, the flux does not fluctuate

TABLE II. List of the equilibrium runs done, with the different sizes and types of systems used in the simulations. The heat capacity is computed through the kinetic energy fluctuations in a microcanonical ensemble.

N	L	N steps	Masses	Heat capacity
100	112	10^6	equal	$0.84-0.89k_B$
200	224	8×10^5	equal	$0.84k_B$
1000	1120	3×10^5	equal	$0.84-0.91k_B$
200	224	7×10^5	different	$0.79-0.88k_B$
200	224	8×10^5	equal[a]	$0.86-0.98k_B$
200	224	8×10^5	different[a]	$0.79k_B$
100	112	10^6	equal[b]	

[a]System with two different interaction potentials, one of every four particles interacting through a repulsive force.
[b]System with an external sinusoidal field.

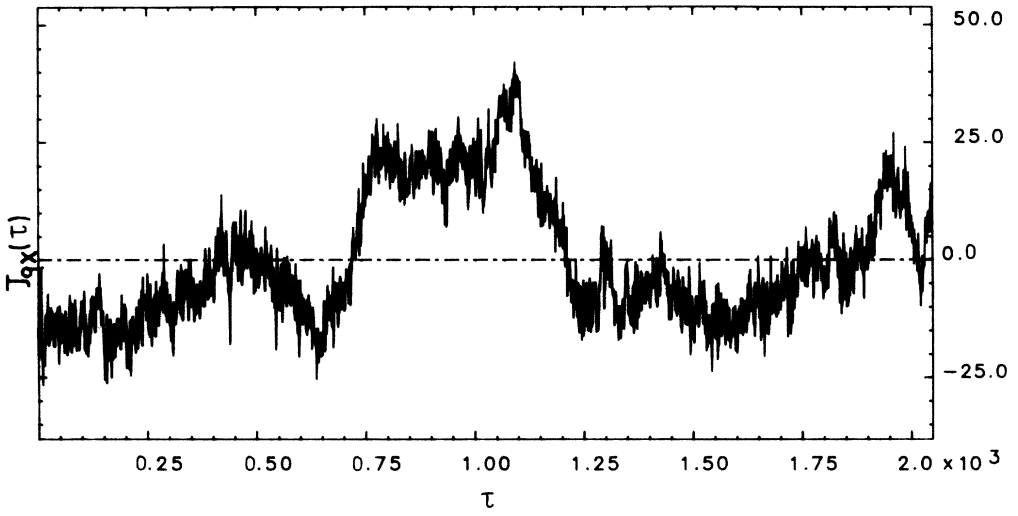

FIG. 5. Heat flux as a function of time for the simple LJ chain. Each point is a time average over 100 time steps.

rapidly around 0, its equilibrium value, but instead it has rapid oscillations around a value which changes only slowly in time. There are two time scales: one, of the order of the relaxation time, corresponds to the rapid decay of the flux around a value which varies on a second time scale. This last time scale is so long that even with runs of a million time steps, the average value of the heat flux was not small compared to the mean-square deviation. The correlation does not decay to zero on short times but rather it remains large for times where the periodic boundary conditions taken start to interfere. After the fluctuating heat flux has propagated through the chain, it becomes self-correlated and the decay is then very slow. This long-time correlation is shown in Figs. 6; in Fig. 6(a) we have plotted the time correlation function on a time interval of 500 time steps. As can be seen, the decay is rapid for short times and then becomes very slow. In Fig. 6(b) we have plotted the long-time correlation function obtained by taking one point on 100; the time interval considered is 100 000 time steps and it is obvious from the figure that the correlation persists for a very long time. We have tried to separate the short-time decay from the longer time scale correlation. This is done in Fig. 7; the correlation function is obtained by successive Fourier transform of signals consisting of 64 (or 256) values whose mean value has been subtracted. One can then average the power spectra and Fourier inverse. This technique is usually used to compute correlation functions in equilibrium molecular dynamics and, of course, is equivalent (but much less costly) to a treatment of the entire signal (which can be 100 000 points long). In our case, however, because the existence of these two time scales, we obtain a completely different result: One can observe on short-time scales a rapid decay of the correlation, which eventually becomes negative. On the contrary, for long times, the heat flux remains correlated. This can be understood from Fig. 5, which shows the time behavior of the heat flux: The average value of the heat flux decreases to zero after a very long time; even after 10^6 time steps, its average is -2.4 and its mean-square displacement is 10.5 (see Table III).

As we already stressed in Sec. I, another one-dimensional model, the "ding-a-ling" chain, is capable of displaying dissipativity in a very convincing way. Therefore one would like to relate the existence of thermodynamic behavior to elementary dynamical processes

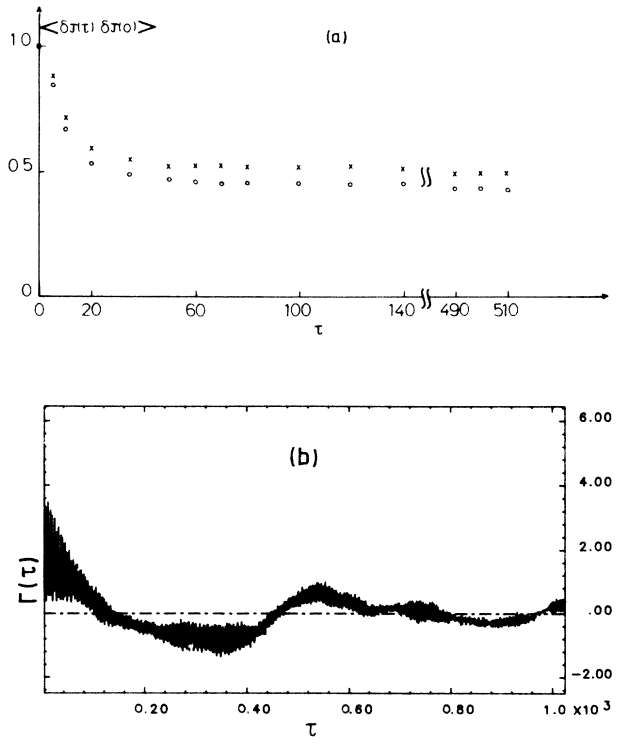

FIG. 6. (a) Heat-flux autocorrelation function for the simple LJ chain ($N = 1000$). (b) Correlation function obtained by taking one point every 100 time steps. The total time considered here then corresponds to 100 000 time steps.

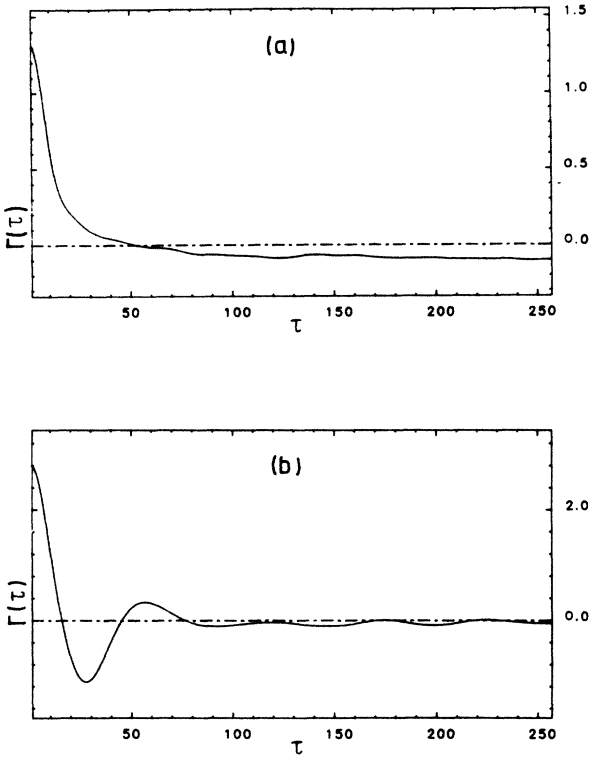

FIG. 7. Short-time correlation function computed by the average of several signals of 256 points. Graph (a) refers to the equal masses case and graph (b) refers to the case with different masses (1 and 10).

that are the collisions. In Sec. III we have shown evidence of the propagation of excitations in the form of soundlike pulses, as in a hard-rod system. The "ding-a-ling" model results from the addition of a chain of hard rods and a chain of harmonic oscillators. Although separately these models have too many constants of the motion to show irreversible behavior, once they are mixed the resulting dynamical behavior is very different from the one of the original models; constants of the motion of the "unperturbed" models are destroyed in such a way that the propagating excitations are rapidly damped. The Lennard-Jones chain can be thought of as a linear assembly of harmonic oscillators being perturbed by anharmonic coupling, and if the anharmonicity is strong enough one expects similar properties as in the "ding-a-ling" model. However, this is not what happens and one could wonder if modifications to the simple chain could possibly lead to a sufficient increase of the anharmonicity. We thought of introducing impurities in the original system: one particle in two has a heavier mass (ten times larger); as shown in Ref. 5, spectral properties of harmonic chains are sensible to the introduction of such impurities. Besides, it has some similarity with hard-rod collisions. This could well give the chain the necessary freedom to spread the excitations. The modification, however, was not successful, as can be seen from Table III; the heat flux still fluctuates on a very-long-time scale and its mean-square displacement is of the same order of magnitude than the mean. The difference in the short-time behavior of the correlation function is shown in Fig. 7(b), where the correlation function has been measured by averages over many small time intervals, as described above; the function here goes to zero.

TABLE III. Mean value and mean-square displacement for the heat flux. (a) for the LJ chain; (b) for the LJ chain with an external field; (c) for the LJ chain with repulsive impurities; (d) for the LJ chain with different masses; (e) for the LJ chain with different masses and repulsive impurities.

(a)	−2.12	15.22
(b)	−0.85	6.75
(c)	7.46	14.28
(d)	−10.52	10.64
(e)	−9.97	10.36

In Fig. 8 we have shown the same short-time behavior for a model where one particle in four has a purely repulsive interaction with its neighbors:

$$V_{\text{impurity}}(x_{ij})=4\epsilon(\sigma/x_{ij})^{12} . \tag{10}$$

The idea here is similar to the different masses model: The introduction of different particles in the chain is expected to favor the spreading of excitations and to lead to a rapid decay of correlations in the heat-flux time evolu-

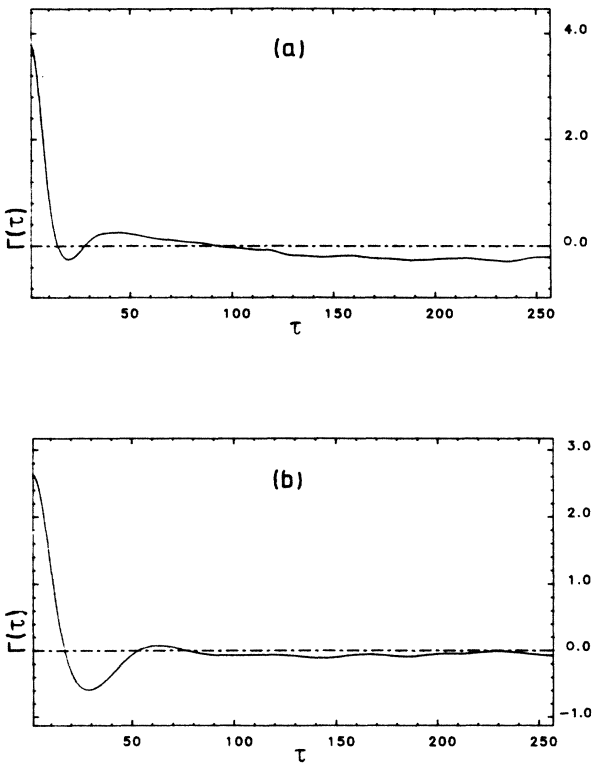

FIG. 8. As in Fig. 7 but with repulsive impurities. Graph (a) is for the equal masses case and graph (b) is for the different masses case.

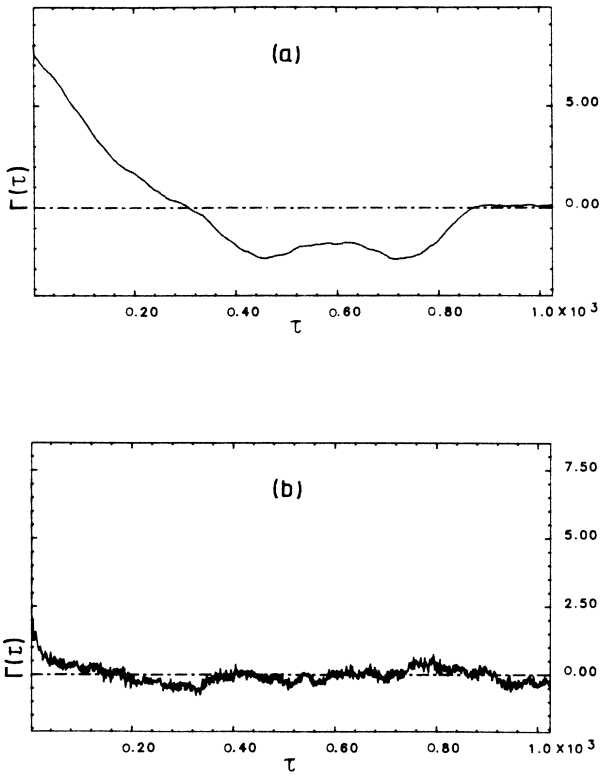

FIG. 9. Long-time correlation function for the LJ chain with (a) equal and (b) different masses in the case of repulsive impurities. As in Fig. 6(b), these curves are obtained by taking one point every 100 steps and then computing the correlation function.

tion. Here also, as can be seen in Figs. 8 and 9, the short-time scale is decoupled from the long time-scale, and for short time one finds an oscillatory relaxation. However, on time scales large with respect to this relaxation time, correlations persist and the time average of the heat flux itself does not reach the expected equilibrium value. It seems that the modified models keep too much similarity with the ideal harmonic chain, where the heat flux is constant, to get rid of this slow decay.

In view of the results obtained in Ref. 14, we also measured the effect of the addition of an external periodic field representing a periodic lattice in the Frenkel-Kontorova model [see Eq. (8)]. As can be seen in Table III, the mean of the heat flux is an order of magnitude lower than the mean-square displacement. The correlation function, however, does not decay to zero on short-time scales, but remains correlated (see Figs. 10 and 11), and it oscillates at a frequency which depends on the amplitude of the field; the frequency goes to zero with V_0. The oscillation comes from the fact that energy is periodically transferred from the particles to the field and back. The anomalous fluctuations do not disappear, which is surprising in view of the result described in Ref. 14.

V. CONCLUSION

The present study raises more questions than it can answer. It presents some numerical results of one-dimensional physical models where the usual thermodynamical behavior is not observed, and the understanding that we have relies more on intuition than on an even nonrigorous, theoretical approach.

The Lennard-Jones fluid is probably the model which has been used with most success in the numerical simulation in three dimensions. Studies in two and one dimensions have been done investigating the stochastic transition which occurs at low energy. Although the trajectories in phase space are chaotic above that threshold, it is not sufficient to ensure thermodynamic behavior. The ability of this chain to transport energy fluctuations in the form of wavelike excitations certainly modifies the mechanisms of dissipativity that are common in transport. The nonequilibrium simulations show that a relaxation occurs locally in the system, with the temperature

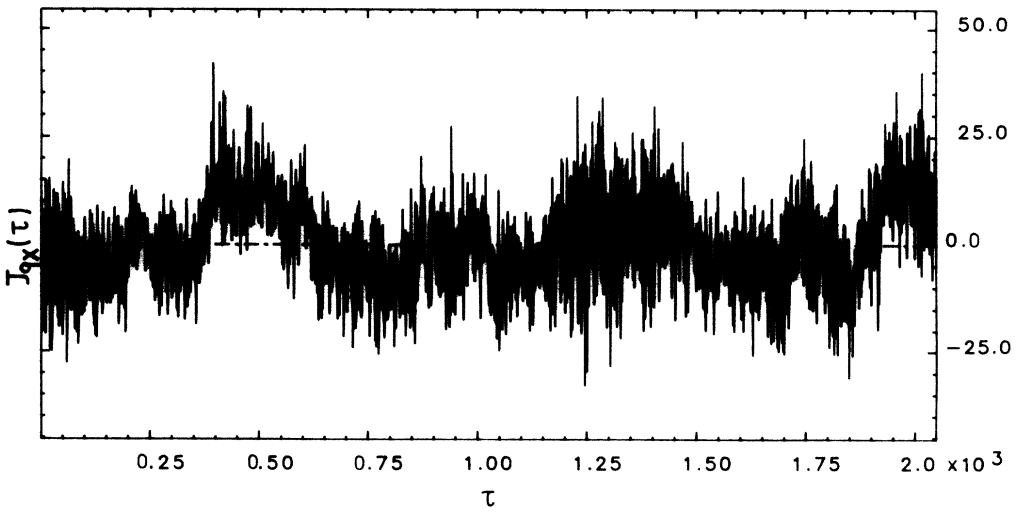

FIG. 10. Heat flux as a function of time in the case of the Lennard-Jones chain submitted to an external field. Each point is an average over 100 time steps.

varying linearly in space. However, the fluctuations of the heat flux in time look more like trajectories generated from nonlinear dynamical systems rather than from fluctuating hydrodynamical ones. A characterization of the chaotic nature of the heat-flux time evolution along the lines developed by nonlinear dynamical systems could give some confirmation of this picture.

One usually looks at anharmonic chains in terms of a perturbation expansion. The heat flux in harmonic chains is constant of the motion and anharmonicity destroys its time invariance, in the same way that collisions in a gas bring the fluid to equilibrium. This was stated in a theorem of Poincaré, which says that invariants of the unperturbed system could not be analytical functions of the perturbation. In one dimension it is known that cubic terms are not sufficiently nonlinear so that this theorem applies. The model studied here shows that this theorem could very well not be valid in the case of Lennard-Jones interactions which contain higher-order terms in the anharmonicity. From this point of view, the "ding-a-ling" model contains a highly nonlinear coupling between the oscillators, which cannot be expanded in anharmonic series.

One may also look at this last model from another point of view, namely an assembly of hard rods perturbed by harmonic strings. When the frequency corresponding to the string is high, the motion becomes chaotic and dissipativity sets in. We have tried to obtain the same behavior in modified Lennard-Jones chains. The changes made have not destroyed the coherent propagation of excitations. The reason for this is probably to be found in the fact that the Lennard-Jones chains miss an essential stochastic ingredient provided by the high-frequency

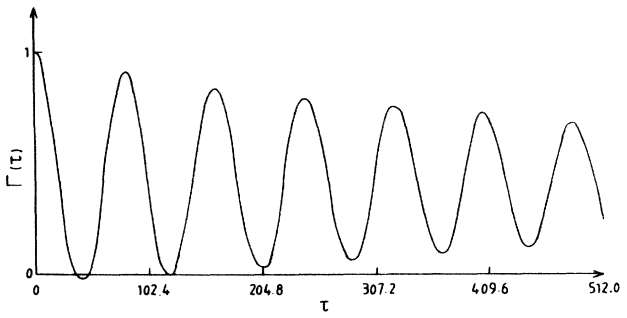

FIG. 11. Time correlation function for the heat flux of the chain in the presence of the field. $V_0 = 10$.

motion of the harmonic strings. Indeed, in a hard-rod chain, energy and velocity transport remain correlated during the propagation along the chain. With high-frequency strings, the system is able to distribute the energy initially put on one particle to a sufficiently large set of particles so as to have local equilibrium. This is, however, not true for low-frequency strings or for the Lennard-Jones chains in which energy and momentum transport remain transported by a group of particles which does not increase with time.

ACKNOWLEDGMENTS

We thank Professor G. Nicolis for encouragement. We are grateful to Professor A. Bellemans for clarifying discussions. Financial support was provided to us by the "Actions de Recherche Concertées" program (M.M.) and by the Ministry of National Education of the Kingdom of Morocco (A.A.).

[1]E. Fermi, J. Pasta, and S. Ulam, *Studies of Non-Linear Problems,* Los Alamos Scientific Laboratory Report No. LA-1940, 1955 (unpublished), reprinted in E. Fermi, *Collected Works of Enrico Fermi* (University of Chicago Press, Chicago, 1965), Vol. II, p. 978.

[2]For a review, see A. M. S. Tremblay, in *Recent Developments in Nonequilibrium Thermodynamics,* edited by J. Casas-Vasquez, D Jou, and J. Lebon (Springer-Verlag, Berlin, 1984).

[3]D. Beysens, Physica A **118**, 250 (1983).

[4]G. Klein and I. Prigogine, Physica (Utrecht) **19**, 1053 (1953); P. Mazur and E. Montroll, J. Math. Phys. **1**, 70 (1960).

[5]A. Casher and J. L. Lebowitz, J. Math. Phys. **12**, 1701 (1971).

[6]R. E. Peierls, Ann. Phys. (Leipzig) **3**, 1055 (1929).

[7]D. M. K. MacDonald, in *Proceedings of the International Symposium on Transport Processes in Statistical Mechanics, Brussels, 1956,* edited by I. Prigonine (Wiley, New York, 1958).

[8]Y. Pomeau and P. Résibois, Phys. Rep. **19**, 63 (1975).

[9]J. Ford and J. Waters, J. Math. Phys. **4**, 1293 (1963).

[10]R. S. Northcote and R. B. Potts, J. Math. Phys. **5**, 383 (1964).

[11]N. J. Zabusky and M. D. Kruskal, Phys. Rev. Lett. **15**, 241 (1965).

[12]E. W. Montroll, in *Lectures in Statistical Physics,* Vol. 28 of *Lectures in Statistical Physics,* edited by W. C. Schieve and J. S. Turner (Springer-Verlag, Berlin, 1974).

[13]M. Casartelli, E. Diana, L. Galgani and A. Scotti, Phys. Rev. A **13**, 1921 (1976).

[14]M. J. Gillan and R. W. Holloway, J. Phys. C **18**, 5705 (1985).

[15]G. Casati, J. Ford, F. Vivaldi, and W. M. Visscher, Phys. Rev. Lett. **52**, 1861 (1984).

[16]F. Mokross and H. Buttner, J. Phys. C **16**, 4539 (1983).

[17]A. Tenenbaum, G. Ciccotti, and R. Gallico, Phys. Rev. A **25**, 2778 (1982).

[18]L. Verlet, Phys. Rev. **159**, 98 (1967).

[19]See Ref. 14, for example.

[20]J. L. Lebowitz, J. K. Percus, and L. Verlet, Phys. Rev. **153**, 250 (1967).

[21]R. Kubo, Rep. Prog. Phys. **29**, 255 (1966).